A Control Lyapunov Function-Based Approach for Particle Nanomanipulation via Optical Tweezers

Melika Golgoon, Alireza Mohammadi[†], and Mark W. Spong

Abstract—Considering the non-affine-in-control system governing the motion of a spherical particle trapped inside an optical tweezer, this paper investigates the problem of stabilization of the particle position at the origin through a control Lyapunov function (CLF) framework. The proposed CLF framework enables nonlinear optimization-based closed-loop control of position of tiny beads using optical tweezers and serves as a first step towards design of effective control algorithms for nanomanipulation of biomolecules. After deriving necessary and sufficient conditions for having smooth uniform CLFs for the optical tweezer control system under study, we present a static nonlinear programming problem (NLP) for generation of robustly stabilizing feedback control inputs. Furthermore, the NLP can be solved in real-time with no need for running computationally demanding algorithms. Numerical simulations demonstrate the effectiveness of the proposed control framework in the presence of external disturbances and initial bead positions that are located far away from the laser beam.

I. INTRODUCTION

Since their introduction by Ashkin [1], optical tweezers (see Figure 1 for its principle of operation) have become one of the primary methods of choice for single-molecule noncontact manipulation studies such as investigation of protein/RNA folding/unfolding and design of molecular motors [2], [3].

One of the enabling factors for dexterous manipulation of target molecules via optical tweezers is the utilization of properly designed control algorithms for positioning of micro/nano-objects (see, e.g., [4]–[11]). However, there are a few challenges that exacerbate the design of closed-loop controllers for optical tweezer-based nanomanipulation. For instance, failure of the optical trapping when particles are located far away from the laser beam, existence of spatially varying and unknown trapping stiffness, and the optical trap Brownian motion, which is induced by thermal noise disturbances, are among these difficulties.

The control Lyapunov function (CLF) framework, thanks to its formal guarantees of stability/safety and the capability of accommodating unmodeled dynamics and parametric uncertainties, appears to be an appealing choice for design of closed-loop control algorithms in optical tweezer-based nanomanipulation tasks. Indeed, CLF-based controllers have

This work is supported by the National Science Foundation (NSF) through the award number CMMI-2153744 and award number CMMI-2153901. M. Golgoon and M. W. Spong are with the Department of Systems Engineering, Erik Jonsson School of Engineering and Computer Science, University of Texas at Dallas, Richardson, TX, USA Email: {melika.golgoon, mspong}@utdallas.edu. A. Mohammadi is with the Department of Electrical and Computer Engineering, University of Michigan-Dearborn, MI, USA Email: amohmmad@umich.edu. †Corresponding Author: A. Mohammadi

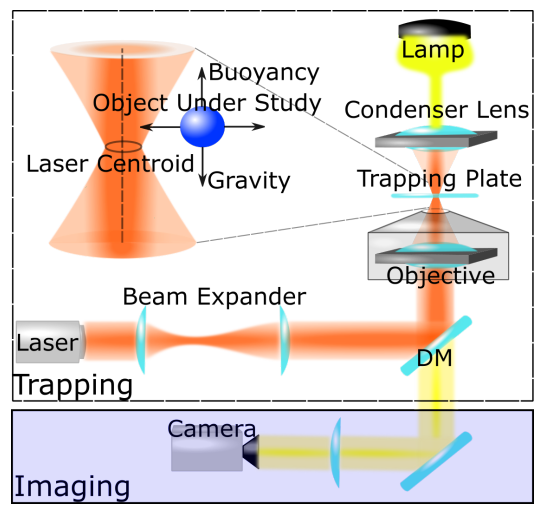


Fig. 1: Schematic of a typical optical tweezer system. The optical tweezer principle of operation is based on utilizing a concentrated laser beam to capture and control individual dielectric particles within a liquid environment. This laser beam, which passes through a microscope objective with a high numerical aperture, serves the dual purpose of trapping and observing the desired particles. By concentrating several milliwatts of laser power at the focal point, trapping forces on the scale of piconewtons can be generated.

been burgeoning in many robotics and autonomous systems applications (see, e.g., [12]–[14]). However, the bulk of these CLF-based closed-loop control applications have concentrated on *control-affine* systems. Furthermore, a difficulty associated with this framework (especially for non-affine-incontrol systems) is the construction of proper CLFs, where one has to rely on computationally expensive and approximate methods such as the sum-of-squares (SOS) programming (see, e.g., [15]) or Zubov's method (see, e.g., [16]). It is of no surprise that *the CLF framework to date has not been utilized for closed-loop control of optical tweezer-based nanomanipulation tasks*.

Prior Literature and Its Gaps. There have been quite a few closed-loop control algorithms proposed for optical tweezer-based nanomanipulation tasks such as a globally asymptotically stabilizing (GAS) control law based on saturation analysis [4], [6], a sliding mode control scheme with adaptive observers [7], a controller with adaptive neural networks [8], a visual servo proportional control law [9], [10], and a Chetaev control framework for protein unfolding [11], to name a few. Given the proliferation of optimization-based

Variable	Value	Variable	Value
m	$5.5 \times 10^{-10} \text{ mg}$	r_p	$1~\mu\mathrm{m}$
β_d	$0.01~\mathrm{pNs/\mu m}$	R	$0.675~\mu\mathrm{m}$
α_3	22 pN/ μ m ³	α_1	$10 \text{ pN/}\mu\text{m}$
R	$0.674~\mu\mathrm{m}$	R_{max}	$0.3893~\mu{\rm m}$

TABLE I: The optical tweezer simulation parameters.

nonlinear controllers such as MPC-based (see, e.g., [17]), optimal decision strategy (ODS)-based (see, e.g., [18], [19]), and CLF-based (see, e.g., [20]) control schemes, which can directly account for stability and safety of the controlled system, such a framework is still missing for control of optical tweezers.

Contributions of the Paper. By developing a CLF framework for the first time in the optical tweezer control literature, this paper contributes to closed-loop control algorithm design for optical tweezer-based nanomanipulation tasks. Considering the non-affine-in-control nanomanipulation control system, we present necessary and sufficient conditions that can be used for generation of smooth CLFs (Proposition 1 and Corollary 1). The obtained CLFs can be employed for generation of robustly stabilizing feedback control inputs via static nonlinear programming problems (NLPs). The obtained NLPs can be solved in real-time with no need for running computationally demanding algorithms. Numerical simulations demonstrate the effectiveness of our CLF-based control algorithms against one of the renowned GAS control laws in the optical tweezer control literature [4], [6].

The rest of this paper is organized as follows. After presenting the model of the optical tweezer control system and formulating our control objectives in Section III, we present our CLF control framework in Section III. Next, we present our simulations in Section IV. Finally, we conclude the paper in Section V with further remarks and future research directions.

II. MODELING AND CONTROL OBJECTIVES

In this section we briefly review the dynamical model of the optical tweezer-based nanomanipulation task under study and present our control objectives.

A. Model

We will use the control oriented model due to Bamieh and collaborators (see, e.g., [4], [6]), where the behavior of tiny beads trapped in a solvent (e.g., water or glycerol) can be described by modeling the optical tweezer force as a nonlinear restoring spring force acting on the beads in accordance with the experimental observations by Simmons *et al.* [21]. The optical tweezer parameters are taken from [4], [6] and provided in Table I. Additionally, following the nanomanipulation literature (see, e.g., [9], [10]), we assume that the gravitational force and the buoyancy force neutralize each other.

The Trapped Particle Equation of Motion. The governing equation of motion for a trapped bead of mass m under the optical trapping force $F_t(\cdot)$, viscous drag force $F_d(\cdot)$,

and external disturbance force $F_e(\cdot)$ due to factors such as thermal noises, is given by

$$m\ddot{x} = F_t(x_r) + F_d(\dot{x}) + F_e(t),$$
 (1)

where the relative position of the bead (i.e., x_r) is determined by the bead lateral position (i.e., x) and the laser focus position (i.e., x_T) according to

$$x_r := x - x_T. \tag{2}$$

In Equation (1), the nonlinear trapping force is given by

$$F_t(x_r) = \varphi(x_r)(\alpha_3 x_r^3 - \alpha_1 x_r), \tag{3}$$

where

$$\varphi(y) := \begin{cases} 1 & \text{for } |y| < R \\ 0 & \text{otherwise.} \end{cases}$$
 (4)

Finally, the viscous drag force $F_d(\cdot)$ is given by

$$F_d(\dot{x}) = -\beta_d \dot{x},\tag{5}$$

where the viscous damping factor of a bead with radius r_p and trapped in a fluid with viscosity η_f is determined by Stoke's equation $\beta_d = 6\pi \eta_f r_p$.

Trap Stiffness. The trap stiffness is given by $\kappa(x) = \frac{dF_t}{dx}$ (note that $\frac{dF_t}{dx} = \frac{dF_t}{dx_r}$ due to the chain rule), where $F_t(x)$ is the trap force given by (3). Consequently, it follows that

$$\left| \frac{dF_t}{dx_r} \right| = \left| \frac{\delta(x_r)}{\beta_d} \left\{ 3\alpha_3 x_r^2 - \alpha_1 \right\} \right|. \tag{6}$$

The right plot in Figure 2 depicts the profile of $\beta_d \cdot |\frac{dF_t}{dx_r}|$ versus the relative position of the bead, i.e., x_r . The trap stiffness becomes equal to the Hookean constant of the optical tweezer, i.e., $\frac{\alpha_1}{\beta_d}$, whenever $x_r = 0$.

The Optical Tweezer Control System. The interplay between inertia and viscous drag dictates the dynamic behavior of particles trapped by the optical tweezer. Owing to the inherent scaling laws governing these forces, microscopic particles confined within a harmonic potential and subjected to low Reynolds number conditions (characterized by slow motion within a viscous medium) experience a predominant influence of viscous drag on their inertial motion (see, e.g., [2] for further details). Consequently, assuming a low Reynolds number regime, where viscous drag dominates inertia, one can neglect the inertial effects and arrive at the following non-affine-in-control control system

$$\dot{x} = f_{\text{twz}}(x, u, F_e), \ x \in \mathbb{R}, \ u \in \mathcal{U}, \ F_e \in \mathcal{D}, \tag{7}$$

where $f_{\text{twz}} : \mathbb{R} \times \mathcal{U} \times \mathcal{D} \to \mathbb{R}$ is the continuous function

$$f_{\text{twz}}(x, u, F_e) := \frac{\varphi(x - u)}{\beta_d} [\alpha_3 (x - u)^3 - \alpha_1 (x - u)] + \frac{F_e}{\beta_d},$$
(8)

and $\mathcal{U} \subset \mathbb{R}$, $\mathcal{D} \subset \mathbb{R}$ are some closed intervals, respectively. Furthermore, the control input u is the laser focus position, namely, $u := x_T$. In (7), the control input can be any measurable locally essentially bounded signal $u(\cdot) : [0, \infty) \to \mathcal{U}$

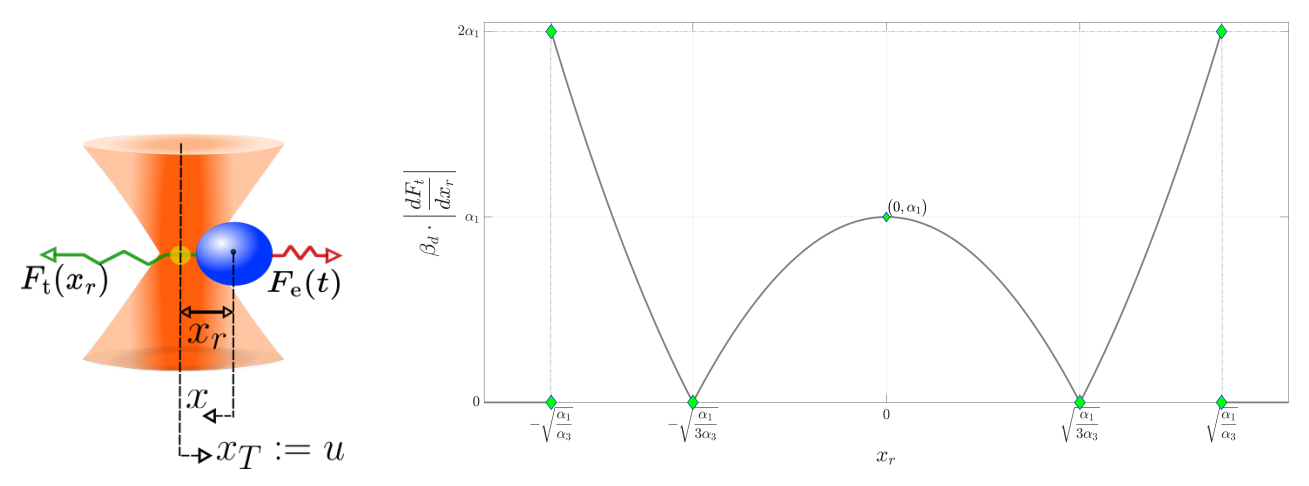


Fig. 2: The optical tweezer and its stiffness: (left) the important variables in the optical tweezer non-affine-in-control control system model; and, (right) the profile of $\beta_d \cdot \left| \frac{dF_t}{dx_r} \right|$ versus x_r .

and the disturbance $F_e(\cdot):[0,\infty)\to\mathcal{D}$ is assumed to be Lebesgue measurable and locally essentially bounded. Finally, the continuity of $f_{\text{twz}}(\cdot)$ implies that the trapping radius R in (4) should satisfy $R=(\frac{\alpha_1}{\alpha_3})^{0.5}$. The left schematic diagram in Figure 2 demonstrates the important variables of the model given by (7) and (8).

B. Control Problem Formulation

Considering the optical tweezer control system in (7), which is non-affine-in-control, our control objective is to robustly stabilize the position of the bead x to the origin by means of a robustly stabilizing feedback input u=k(x) in the presence of measurement errors $e(\cdot)$ and external disturbances $F_e(\cdot)$. In particular, we consider

$$\dot{x}(t) = f_{\text{twz}}(x(t), k(x(t) + e(t)), F_e(t)),$$
 (9)

which is the control system in (7) under the state feedback control law u=k(x), sensor measurement error e(t), and external disturbance $F_e(t)$.

We would like to find a robustly stabilizing feedback (following Ledyaev and Sontag [22], [23]) that is robust with respect to measurement errors $e(\cdot)$ and external disturbances $F_e(\cdot)$ in the sense that it drives all the states of the perturbed system (9) to a small neighborhood of the origin.

III. CLF-BASED CONTROL ALGORITHM

In this section we present our solution to the control problem formulated in Section II, which is based on the notion of smooth CLFs and generation of CLF-based robustly stabilizing feedback control inputs due to Ledyaev and Sontag (see, e.g., [22], [23]). We first provide necessary and sufficient conditions for having smooth CLFs for optical tweezers in Section III-A. Next, we present our CLF-based control algorithm in Section III-B.

A. Construction of Smooth CLFs for the Optical Tweezer Control System

Consider the non-affine-in-control nonlinear control system (7) with no disturbance input, i.e., when $F_e=0$. A differentiable function $V:\mathbb{R}\to\mathbb{R}_{\geq 0}$ is said to be a smooth control Lyapunov function (CLF) for the unperturbed optical tweezer control system (7) with $F_e=0$ if $V(\cdot)$ is positive definite, proper, and infinitesimally decreasing in the sense that there exists a positive definite continuous function $W:\mathbb{R}\to\mathbb{R}_{\geq 0}$ and some nondecreasing function $\sigma:\mathbb{R}_{\geq 0}\to\mathbb{R}_{\geq 0}$, such that

$$\sup_{x \in \mathbb{R}} \min_{|u| \le \sigma(|x|)} \nabla V(x) \cdot f_{\text{twz}}(x, u, 0) + W(x) \le 0. \quad (10)$$

Remark 1: From a theoretical perspective, the constraint $|u| \le \sigma(|x|)$ in the definition of differentiable CLFs rules out the possibility of unbounded control inputs u(t) near the origin (see, e.g., [22] for further details).

The following proposition provides a necessary and sufficient condition for having differentiable CLFs for the optical tweezer control system.

Proposition 1: Consider the optical tweezer control system (7). Given a positive definite continuous function $W: \mathbb{R} \to \mathbb{R}_{\geq 0}$, a smooth function $V: \mathbb{R} \to \mathbb{R}_{\geq 0}$ is a differentiable CLF satisfying (10) if and only if

$$W(x) - \zeta_0 \left| \frac{dV}{dx} \right| \le 0$$
, for all $x \in \mathbb{R}$, (11)

where
$$\zeta_0 := \frac{2\sqrt{3}}{9\beta_d}R\alpha_1$$
.

Proof: Considering the given function $W(\cdot)$, we define the mapping $G: \mathbb{R} \times \mathbb{R} \to \mathbb{R}$, $(x,u) \mapsto \nabla V(x) \cdot f_{\text{twz}}(x,u,0) + W(x)$, where $V(\cdot)$ is some differentiable

function with derivative $\frac{dV(x)}{dx}$. Therefore,

$$G(x,u) = \left(\frac{dV}{dx}\right) \cdot \frac{\varphi(x-u)}{\beta_d} P(x-u) + W(x), \quad (12)$$

where $P(x-u) := \alpha_3(x-u)^3 - \alpha_1(x-u)$ and W(x) is some positive definite and continuous function. It follows from (10) that $V(\cdot)$ is a differentiable CLF for the unperturbed optical tweezer system if and only if

$$\min_{|u| \le \sigma(|x|)} G(x, u) \le 0 \text{ for all } x \in \mathbb{R}. \tag{13}$$

where $\sigma: \mathbb{R}_{\geq 0} \to \mathbb{R}_{\geq 0}$ is some nondecreasing function. We consider an arbitrary $x \in \mathbb{R}$ and the mapping $H: \mathbb{R} \to \mathbb{R}$, $u \mapsto G(x,u)$. Considering the compact interval $\mathcal{I}_x := [-\sigma(|x|), \sigma(|x|)]$, it can be seen that the inequality given by (13) holds if and only if

$$\min_{u \in \mathcal{I}_x} H(u) \le 0 \text{ for all } x \in \mathbb{R}. \tag{14}$$

Since H(u) is a continuous function, it attains its global minimum on the compact interval \mathcal{I}_x for each given $x \in \mathbb{R}$. The critical points of $H(\cdot)$, where $\frac{dH}{du} = 0$, are $u_1^* = x - (\frac{\alpha_1}{3\alpha_3})^{0.5}$ and $u_2^* = x + (\frac{\alpha_1}{3\alpha_3})^{0.5}$, respectively. At these points, we have

$$H(u_{1,2}^*) = W(x) \pm \underbrace{\frac{2\sqrt{3}}{9\beta_d}R\alpha_1}_{\zeta_0}\frac{dV}{dx}.$$
 (15)

Considering the boundary points of the interval \mathcal{I}_x , namely, $u_l = -\sigma(|x|)$ and $u_r = \sigma(|x|)$, we define $\kappa_r(x) := \frac{\varphi(x-u_r)}{\beta_d} P(x-u_r)$ and $\kappa_l(x) := \frac{\varphi(x-u_l)}{\beta_d} P(x-u_l)$. Hence, we have

$$\min_{u \in \mathcal{I}_x} H(u) = W(x) + \min \left\{ \pm \zeta_0 \frac{dV}{dx}, \kappa_r(x) \frac{dV}{dx}, \kappa_l(x) \frac{dV}{dx} \right\}.$$
(16)

Therefore, it immediately follows that

$$\min_{u \in \mathcal{I}_x} H(u) \le W(x) - \zeta_0 \left| \frac{dV}{dx} \right|. \tag{17}$$

The proof follows from replacing (17) in Inequality (14).

Remark 2: As it can be seen from Proposition 1, the physical parameters of the optical tweezer, i.e., the trapping radius, the environment viscous damping factor, and the trap stiffness coefficients, directly appear in the condition given by (11).

One can now utilize Proposition 1 to generate a plethora of smooth CLFs for the optical tweezer non-affine-in-control nonlinear control system. For instance, it can be immediately seen that the pair

$$W(x) = |x|, \ V(x) = \frac{1}{2\ell}x^2,$$
 (18)

in which ζ is a positive constant, with $0 < \zeta \le \zeta_0$, satisfy the condition given by Proposition 1 and therefore $V_1(\cdot)$ is a smooth CLF for the optical tweezer control system.

It is sometimes desirable to directly control the rate of decay of CLFs (see, e.g., [24]). The following corollary, which is a direct result of Proposition 1, addresses the issue of the control of the rate of decay of CLFs.

Corollary 1: Consider the statement of Proposition 1. Moreover, consider

$$W(x) = \frac{1}{\zeta} \gamma(x) V(x),$$

$$V(x) = V_0 \left\{ \exp\left(\int_0^x \frac{\gamma(s)}{\zeta} ds\right) - 1 \right\},$$
(19)

where $\gamma: \mathbb{R} \to \mathbb{R}_{\geq 0}$ is any continuous function with $\gamma(x) > 0$ for all x in $\mathbb{R}\setminus\{0\}$ and $\gamma(0) \geq 0$, V_0 is an arbitrary positive constant, and ζ is a positive constant, where $0 < \zeta \leq \zeta_0$. Then, $V(\cdot)$ is a smooth CLF for the optical tweezer.

As special examples of Corollary 1, if $\gamma_1(x)=|x|$ and $\gamma_2(x)=\gamma_0$ with $\gamma_0>0$ a positive constant, then

$$V_1(x) = V_0 \left\{ \exp\left(\frac{x^2}{2\zeta}\right) - 1 \right\}, \text{ and}$$

$$V_2(x) = V_0 \left\{ \exp\left(\frac{\gamma_0 x}{\zeta}\right) - 1 \right\},$$
(20)

are smooth CLFs for the optical tweezer control system corresponding to $\gamma_1(\cdot)$ and $\gamma_2(\cdot)$, respectively.

B. CLF-based Robust Stabilizing Feedback for the Optical Tweezer with Constraints on Laser-Induced Heating

In this section we provide a formal CLF-based closed-loop control synthesis method to directly address this issue.

Once a smooth CLF for the unperturbed optical tweezer control system with no disturbance input is found, then the feedback input $u=k^{*}(x)$ satisfying the steepest descent relationship

$$k^*(x) := \underset{|u| \le \sigma(|x|)}{\operatorname{argmin}} W(x) + \nabla V(x) \cdot f_{\text{twz}}(x, u, 0), \quad (21)$$

will be a globally asymptotically stabilizing (GAS) feedback for the optical tweezer perturbed system (9) with sensor measurement errors and external disturbances according to [22, Theorem 7].

The following proposition, which directly utilizes the proof of Proposition 1, removes the need for running an optimization algorithm for finding the steepest descent feedback law in (21).

Proposition 2: Assume that $V(\cdot)$ is a given differentiable CLF for the optical tweezer non-affine-in-control system given by (7). Then, the steepest descent feedback control input satisfying (21) can be found from

$$k^*(x) = \underset{u \in \left\{x \pm \left(\frac{\alpha_1}{3\alpha_3}\right)^{0.5}, \pm \sigma(|x|)\right\}}{\operatorname{argmin}} W(x) + \nabla V(x) \cdot f_{\text{twz}}(x, u, 0).$$
(22)

Proof: The proof follows in a straightforward manner from the proof of Porposition 1. Specifically, consider any arbitrary position $x \in \mathbb{R}$. Then, the feedback input u^* , which minimizes G(x, u) in (12) on the compact interval

 $\mathcal{I}_x = [-\sigma(|x|), \, \sigma(|x|)],$ is either one of the critical points $x \pm (\frac{\alpha_1}{3\alpha_3})^{0.5}$ or one of the boundary points $\pm \sigma(|x|)$.

Remark 3: Thanks to the special structure of the non-affine-in-control optical tweezer nonlinear control system, there is no need for running computationally demanding optimization schemes for solving the NLP in (22). Indeed, due to Proposition 2, the robust stabilizing feedback $k^*(x)$ can be computed by checking *only four* values at each bead position.

IV. SIMULATION STUDIES

In this section we present the numerical simulations that demonstrate the effectiveness of the proposed control framework in the presence of external disturbances. The optical tweezer simulation parameters are taken from [4], [6] and provided in Table I.

A particle trapped within an optical tweezer experiences an external random thermal Langevin force $F_e(t)$, which acts as an external disturbance in the control system dynamics given by (8). This force has an average of zero, i.e., $\langle F_e(t) \rangle = 0$, and possesses a constant power spectrum equal to $4\beta k_B T$, where k_B is Boltzmann's constant and T represents the absolute temperature [25]. For a bead with $r_p = 1\mu m$, the power spectrum is approximately $1.6 \times 10^{-4}~\mu m^2$ at room temperature.

We first consider a globally asymptotically stabilizing (GAS) control law due to Bamieh and collaborators [4], [6]. This control law is given by

$$k(x) = x - \omega \tanh\left(\frac{p}{\lambda \beta_d}x\right),\tag{23}$$

where p=10, $\lambda=5$, and $\omega=0.3893\,\mu\mathrm{m}$. The control law given by (23) is obtained from approximating the trapping force by a hypberbolic tangent function (see [4], [6] for further details).

Figure 3 demonstrates the bead position time-profile starting from $x(0)=1~\mu\mathrm{m}$ while applying the control law given by (23). The inner plot demonstrates the time profile of the optical trap stiffness. As it can be seen from the two plots, both the commanded control input x_T and the trap stiffness $|\frac{dF_t}{dx}|$ oscillate widely to stabilize the bead position. Another notable issue is the sharp variation in the control input and the trap stiffness time profiles starting from instance $t\approx 3.9~\mathrm{ms}$. The observed trap stiffness oscillations are in accordance with the profile depicted in the left plot in Figure 2. Specifically, an oscillatory bead relative position about the origin gives rise to stiffness oscillations about $\frac{\alpha_1}{\beta_d}$.

In the second set of numerical simulations, we consider the CLF pair V(x) and W(x) given by (19) with $\zeta = \zeta_0$. Furthermore, we constrain the optical trap stiffness by setting $\kappa_0 = \alpha_1$, which results in $\sigma_T(|x|) = |x|$. The stabilizing control input is then generated by considering the NLP given by (21). It is remarked that the NLP in (21) does not require any knowledge of the external disturbances and is generated by setting $F_e = 0$.

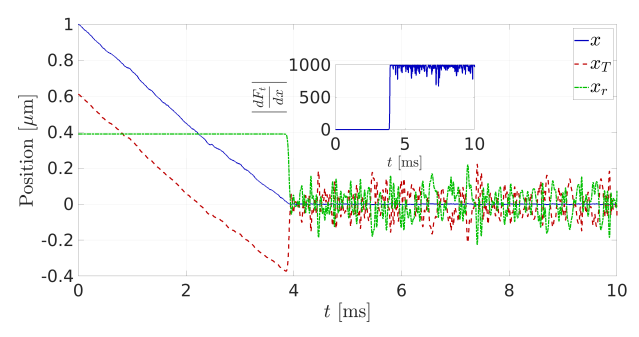


Fig. 3: Stabilization of the position of the bead with initial position $x(0)=1\,\mu\mathrm{m}$ using the optical tweezer and under the GAS control law provided by [4]. The bead is subject to an external random thermal Langevin force of zero average and a power spectrum approximately equal to $1.6\times10^{-4}\,\mu\mathrm{m}^2$. The inner plot depicts the time-profile of the optical tweezer trap stiffness.

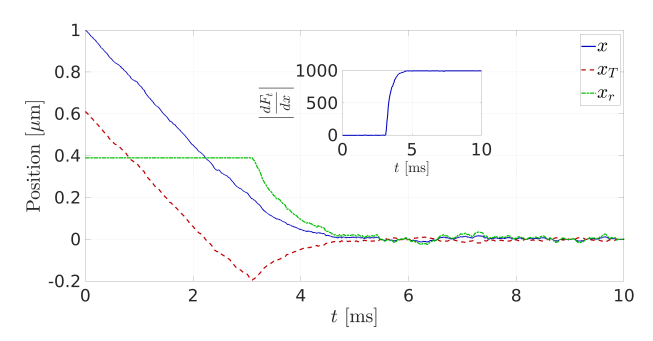


Fig. 4: Stabilization of the position of the bead with initial position $x(0)=1\,\mu\mathrm{m}$ using the optical tweezer and under the proposed control law in this paper. The bead is subject to an external random thermal Langevin force of zero average and a power spectrum approximately equal to $1.6\times10^{-4}\,\mu\mathrm{m}^2$. The inner plot depicts the time-profile of the optical tweezer trap stiffness.

Figure 4 demonstrates the bead position time-profile starting from $x(0)=1~\mu\mathrm{m}$ while applying the control law given by (21) with the CLF pair (19) with $\zeta=\zeta_0$. The inner plot demonstrates the time profile of the optical trap stiffness. As it can be seen from the two plots, both the commanded control input x_T and the trap stiffness $|\frac{dF_t}{dx}|$ undergo very small oscillations while managing to drive the bead position to a small neighborhood of the origin. Another notable fact is the smooth behavior of the trap stiffness time profile in comparison with the GAS control law (compare Figure 4 against Figure 3).

From a control system bandwidth requirement perspective, the proposed CLF-based control algorithm is superior with respect to the ad-hoc controller given by (23). As noted by Sehgal *et al.* [26], there are serious limitations for control of the position of the bead (from a bandwidth perspective) when the applied force in optical tweezers has high frequency content.

V. CONCLUSION

This paper examined a control system for a spherical particle within an optical tweezer and explored the challenge of stabilizing the particle's position. This is accomplished using a framework based on a CLF approach, which enables the application of nonlinear optimization-based closed-loop control, for manipulating minuscule beads with optical tweezers. By establishing the necessary and sufficient conditions for the existence of smooth and uniform CLFs within the considered optical tweezer control system, the paper introduced an NLP, which was utilized to generate robustly stabilizing feedback control inputs. Numerical simulations demonstrated the effectiveness of the proposed control approach, even when subjected to external disturbances and initial bead positions positioned far from the laser beam.

Thermal effects can degrade the optical trapping performance due to heating and damage the cells and biomolecules under study. Additionally, increasing the trapping laser power for faster manipulation can lead to undesirable heating effects resulting in induction of thermal stress [27]–[29]. Future research will include design of efficient control algorithms for precise handling of biomolecules (e.g., protein, RNA, and DNA molecules) at the nanoscale and benchmarking the control algorithm performance in advanced optical tweezer simulators such as the OTT toolbox [30]. Another research direction emanating from this work is extending the proposed CLF framework for solving the challenging problem of feedback cooling of optically trapped nanoparticles in high vacuum [31].

REFERENCES

- [1] A. Ashkin, "Applications of laser radiation pressure," Science, vol. 210, no. 4474, pp. 1081–1088, 1980.
- [2] C. Bustamante, L. Alexander, K. Maciuba, and C. M. Kaiser, "Single-molecule studies of protein folding with optical tweezers," *Annu. Rev. Biochem.*, vol. 89, pp. 443–470, 2020.
- [3] C. J. Bustamante, Y. R. Chemla, S. Liu, and M. D. Wang, "Optical tweezers in single-molecule biophysics," *Nat. Rev. Methods Primers*, vol. 1, no. 1, p. 25, 2021.
- [4] A. Ranaweera, B. Bamieh, and A. R. Teel, "Nonlinear stabilization of a spherical particle trapped in an optical tweezer," in 42nd IEEE Conf. Decis. Contr. (CDC). IEEE, 2003, pp. 3431–3436.
- [5] A. Ranaweera, K. Astrom, and B. Bamieh, "Lateral mean exit time of a spherical particle trapped in an optical tweezer," in 2004 43rd IEEE Conf. Dec. Contr. (CDC). IEEE, 2004, pp. 4891–4896.
- [6] A. Ranaweera and B. Bamieh, "Modelling, identification, and control of a spherical particle trapped in an optical tweezer," *Int. J. Robust Nonlin. Contr.*, vol. 15, no. 16, pp. 747–768, 2005.
- [7] X. Li, C. C. Cheah, S. Hu, and D. Sun, "Dynamic trapping and manipulation of biological cells with optical tweezers," *Automatica*, vol. 49, no. 6, pp. 1614–1625, 2013.
- [8] X. Li and C. C. Cheah, "Stochastic optical trapping and manipulation of a micro object with neural-network adaptation," *IEEE/ASME Trans. Mechatron.*, vol. 22, no. 6, pp. 2633–2642, 2017.
- [9] X. Zhang, L. W. Rogowski, and M. J. Kim, "3D micromanipulation of particle swarm using a hexapole magnetic tweezer," in 2019 IEEE/RSJ Int. Conf. Intelli. Robot. Syst. (IROS). IEEE, 2019, pp. 1581–1586.
- [10] —, "Closed-loop control using high power hexapole magnetic tweezers for 3D micromanipulation," J. Bionic Eng., vol. 17, pp. 113– 122, 2020.
- [11] A. Mohammadi and M. W. Spong, "Chetaev instability framework for kinetostatic compliance-based protein unfolding," *IEEE Contr. Syst. Lett.*, vol. 6, pp. 2755–2760, 2022.

- [12] R. Kubo, Y. Fujii, and H. Nakamura, "Control Lyapunov function design for trajectory tracking problems of wheeled mobile robot," *IFAC-PapersOnLine*, vol. 53, no. 2, pp. 6177–6182, 2020.
- [13] K. Galloway, K. Sreenath, A. D. Ames, and J. W. Grizzle, "Torque saturation in bipedal robotic walking through control Lyapunov functionbased quadratic programs," *IEEE Access*, vol. 3, pp. 323–332, 2015.
- [14] A. J. Taylor, V. D. Dorobantu, H. M. Le, Y. Yue, and A. D. Ames, "Episodic learning with control Lyapunov functions for uncertain robotic systems," in 2019 IEEE/RSJ Int. Conf. Intelli. Robot. Syst. (IROS). IEEE, 2019, pp. 6878–6884.
- [15] R. Furqon, Y.-J. Chen, M. Tanaka, K. Tanaka, and H. O. Wang, "An SOS-based control Lyapunov function design for polynomial fuzzy control of nonlinear systems," *IEEE Trans. Fuzzy Syst.*, vol. 25, no. 4, pp. 775–787, 2016.
- [16] F. Camilli, L. Grüne, and F. Wirth, "Control Lyapunov functions and Zubov's method," SIAM J. Contr. Optim., vol. 47, no. 1, pp. 301–326, 2008
- [17] W. Chi, X. Jiang, and Y. Zheng, "A linearization of centroidal dynamics for the model-predictive control of quadruped robots," in 2022 Int. Conf. Robot. Autom. (ICRA). IEEE, 2022, pp. 4656–4663.
- [18] A. Mohammadi and M. W. Spong, "Integral line-of-sight path following control of magnetic helical microswimmers subject to step-out frequencies," *Automatica*, vol. 128, p. 109554, 2021.
- [19] ——, "Quadratic optimization-based nonlinear control for protein conformation prediction," *IEEE Contr. Syst. Lett.*, vol. 6, pp. 373–378, 2022.
- [20] A. Reed, G. O. Berger, S. Sankaranarayanan, and C. Heckman, "Verified path following using neural control Lyapunov functions," in *Conf. Robot Learn.* PMLR, 2023, pp. 1949–1958.
- [21] R. M. Simmons, J. T. Finer, S. Chu, and J. A. Spudich, "Quantitative measurements of force and displacement using an optical trap," *Biophys. J.*, vol. 70, no. 4, pp. 1813–1822, 1996.
- [22] E. D. Sontag, Stability and Feedback Stabilization. New York, NY: Springer New York, 2009, pp. 8616–8630. [Online]. Available: https://doi.org/10.1007/978-0-387-30440-3_515
- [23] Y. S. Ledyaev and E. D. Sontag, "A Lyapunov characterization of robust stabilization," *Nonlinear Anal.*, vol. 37, no. 7, pp. 813–840, 1999.
- [24] W. Tang and P. Daoutidis, "A bilevel programming approach to the convergence analysis of control-lyapunov functions," *IEEE Trans. Automat. Contr.*, vol. 64, no. 10, pp. 4174–4179, 2019.
- [25] F. Gittes and C. F. Schmidt, "Thermal noise limitations on micromechanical experiments," *Eur. Biophys. J.*, vol. 27, pp. 75–81, 1998.
- [26] H. Sehgal, T. Aggarwal, and M. V. Salapaka, "High bandwidth force estimation for optical tweezers," *Appl. Phys. Lett.*, vol. 94, no. 15, 2000
- [27] J. E. Melzer and E. McLeod, "Fundamental limits of optical tweezer nanoparticle manipulation speeds," ACS Nano, vol. 12, no. 3, pp. 2440–2447, 2018.
- [28] A. Blázquez-Castro, "Optical tweezers: Phototoxicity and thermal stress in cells and biomolecules," *Micromachines*, vol. 10, no. 8, p. 507, 2019.
- [29] J. Zenteno-Hernandez, J. V. Lozano, J. Sarabia-Alonso, J. Ramírez-Ramírez, and R. Ramos-García, "Optical trapping in the presence of laser-induced thermal effects," *Opt. Lett.*, vol. 45, no. 14, pp. 3961–3964, 2020.
- [30] T. A. Nieminen, V. L. Loke, A. B. Stilgoe, G. Knöner, A. M. Brańczyk, N. R. Heckenberg, and H. Rubinsztein-Dunlop, "Optical tweezers computational toolbox," *J. Opt. A: Pure Appl. Opt.*, vol. 9, no. 8, p. S196, 2007.
- [31] J. Gieseler, L. Novotny, and R. Quidant, "Thermal nonlinearities in a nanomechanical oscillator," *Nature Phys.*, vol. 9, no. 12, pp. 806–810, 2013.